Evaluation the Effectiveness of the Infrared Flare with a Tactic of Dispensing in Burst

YiFan Hu, BiFeng Song

Abstract—**This study aims to evaluate the effectiveness of infrared (IR) flare against an IR missile with a tactic of dispensing in burst. Firstly, the models of aircraft motion, flare radiation and motion, and missile guidance are described. Secondly, the simulation process is built based on revised guidance loop considering three models, and two criteria to evaluate the effects of flares are given. Lastly, the three-dimensional flight simulations are accomplished. The miss distances due to flare dispensing range at different time intervals are plotted and analyzed. The results show that to achieve effective decoy on IR missile, the flares could be dispensed automatically at an optimum time interval, which is slightly smaller than flare burn time, or dispensed manually in the effective dispensing region at time interval near zero.**

I. Introduction

INFRARED (IR) flares are used to protect the aircraft from a heat-seeking missiles. Deploying infrared flares is the most effective and inexpensive feature against IR missile. There are many methods and tools developed by different specialists [1]-[5]. These papers present the framework to evaluate infrared countermeasure (IRCM) effectiveness. These studies are mainly based on simulation, aiming at deriving the most likely IRCM response by modeling a large number of entities and functions, including IR seeker operation behavior and function, IR signature of the aircraft and flare, dynamic behavior of the aircraft, IRCM and so on. Although these methods are universal to evaluate the effect of different infrared countermeasures, for a designer, a large number of simulations can not be utilized directly. So the results should be analyzed to summarize some principles to assist the design and usage of flares.

As a manner of deploying, dispensing in burst refers to dispensing flare one by one with a time interval. This paper utilizes computer simulation in real time to evaluate the effectiveness of flares with different time intervals.

The paper is organized as follows: Section 2, 3, and 4 describes the aircraft model, the flare model, and the missile model, respectively, which are three top level systems for flight simulation. Section 5 introduces the process and scenario of simulation, and proposes two criteria to evaluate the effectiveness of flares with a tactic of dispensing in burst. Section 6 gives the example and analyzes the results. The final section presents conclusions and suggestions.

Manuscript received December 20, 2009. YiFan Hu is with the School of Aeronautics, Northwestern Polytechnical University, Xi'an, Shaanxi 710072 P.R.China. (phone: 86-029-88486602; e-mail: cherry_hyf@mail.nwpu.edu.cn).

BiFeng Song, is with the School of Aeronautics, Northwestern Polytechnical University, Xi'an, Shaanxi 710072 P.R.China. (e-mail: bfsong@nwpu.edu.cn).

II. Aircraft Model

Suppose that an aircraft is flying in free space with velocity V_t. A local coordinate system is attached to the center of the flying aircraft, and the x and y axes are pointing to the nose and the left wing tip of the aircraft, respectively. It is assumed that the angle of attack of the aircraft is zero, and then the local x axis is coincident with the aircraft velocity V_t.

The aircraft motion in three-dimensional space can be expressed as

$$\begin{aligned} \dot{X}_t &= V_t \cos\theta \cos\psi \\ \dot{Y}_t &= V_t \cos\theta \sin\psi \\ \dot{Z}_t &= V_t \sin\theta \end{aligned} \quad , \tag{1}$$

where $\dot{X}_t$, $\dot{Y}_t$, $\dot{Z}_t$ represent three components of velocity V_t in the global X, Y, Z axes; the azimuthal angle ψ is counterclockwise from X axis to the projection of V_t on to the (X,Y) plane, and $0\text{deg} \le \psi \le 360\text{deg}$; the elevation angle θ is measured from the (X,Y) plane to V_t, and $-90\text{deg} \le \theta \le 90\text{deg}$.

Without considering atmospheric attenuation, the IR radiation intensity of the aircraft in the band of IR sensor is denoted by I_t in unit W/sr.

III. Flare Model

A. Radiation Characteristic

The dominant radiation characteristics which are important to evaluate the effectiveness of the flare include [6]:

1) Spectral characteristic.

2) Radiation intensity. The flare radiation intensity varies with time. The burn time is t_{LAST}, and the burning process can be simplified as three phases [5]. First, after the flare is dispensed from the aircraft and ignited, the infrared radiation intensity rises quickly, and reaches peak intensity I_{MAX} after time t_{TOP}. Then the maximum intensity lasts t_{MAX}. At last, the intensity decreases to zero gradually.

B. Motion Characteristic

The motion characteristic depends on flare's aerodynamic characteristic, which contributes to determine the trajectory of a flare after it separates from the aircraft.

Assume that the velocity of the flare at time t is $v_f(t)$. After the flare is dispensed from the aircraft, it suffers gravity and aerodynamic drag. The direction of aerodynamic drag is

978-1-4244-6044-1/10/$26.00 ©2010 IEEE

opposite to the flare velocity, and the magnitude of drag acceleration can be given by [6]

$$a_d(t) = \frac{C_d A_{ref} \rho_a g v_f(t)^2}{2W(t)} \quad , \tag{2}$$

where C_d is the drag coefficient, A_{ref} is the reference area for the drag coefficient, g is the gravitational acceleration constant, ρ_a is the atmosphere density, $W(t)$ is the flare weight. A typical flare consumes its fuel at a rate of more than 100g/s.

C. Dispenser Parameters

Flare dispenser is the device to eject the flares, which is set on the aircraft. The dispenser parameters include: position, direction, and dispensing velocity. They can not be changed after the aircraft is designed and manufactured.

If a flare dispenser is located at (x_f, y_f, z_f) in the local coordinate system centered at the aircraft, the initial position of flare trajectory in the global coordinate system can be determined. Furthermore, according to the angle with which the dispenser is mounted on the aircraft, the flare launch speed $v_f(0)$ and direction can be derived, which is denoted by an azimuth angle ψ_{vf} and an elevation angle θ_{vf} in the local (aircraft) coordinate system. ψ_{vf} and θ_{vf} have the same definition with ψ and θ in Eq.(1).

D. Tactical Parameters

There are three parameters about the tactical deployment of flares, including: 1) number of flares per dispensing, 2) time interval between each dispensing; 3) dispensing range, which is the distance between the aircraft and the missile when the aircraft starts releasing flares.

According to the number and time interval of deployment, the dispensing manners of flares can be classified as to categories: dispensing in burst, which means dispensing flares one by one at time intervals; salvo, a special situation of dispensing in burst, which represents dispensing flares almost simultaneously in a very short period of time.

All of these tactical parameters can be chosen fully automatically, semi-automatically or manually, based on the threat warning information from missile warning receiver.

IV. Missile Guidance Model

A typical IR missile block diagram is presented in Fig.1, which employs proportional navigation to intercept the target [7]-[9].

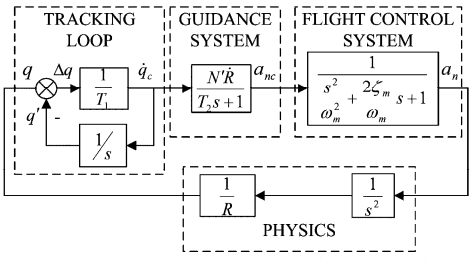

Fig. 1. A simple proportional navigation homing guidance loop

The angle Δq between the IR seeker optical axis and the seeker-to-target line of sight (LOS) is sent into the detecting system as the input. The detecting system outputs the corresponding error signal, which is sent into the tracking mechanism to drive the seeker, making the tracking loop close. However, the tracking process stops when the target is no longer in the instantaneous field of view (IFOV) for some time due to the limitation of IFOV angle. If the track is lost, the missile returns to the search mode after a pre-defined dead-reckon time has expired.

The acceleration command a_{nc} is generated from the output of the seeker based on proportional navigation law, and demodulated to drive the missile control surfaces as commanded by autopilot to achieve the desired acceleration level a_n.

The motion of the missile is calculated according to the kinematics equations, and is taken as the feedback which is inputted to the seeker to make the guidance loop of the missile close.

V. Simulation

A. Flight Simulation

For an amplitude modulation (AM) IR seeker, it tends to average the signal from multiple targets. Hence the optical axis directs towards the centre of gravity of the IR radiation intensity within each exposure [9].

Infrared flares are aimed at deceiving or disrupting the seeker tracking function, and subsequently affecting the missile guidance function. So the revised flight simulation is built by introducing the flares as possible targets into the tracking loop. The following flow chart shows the detailed steps of the simulation.

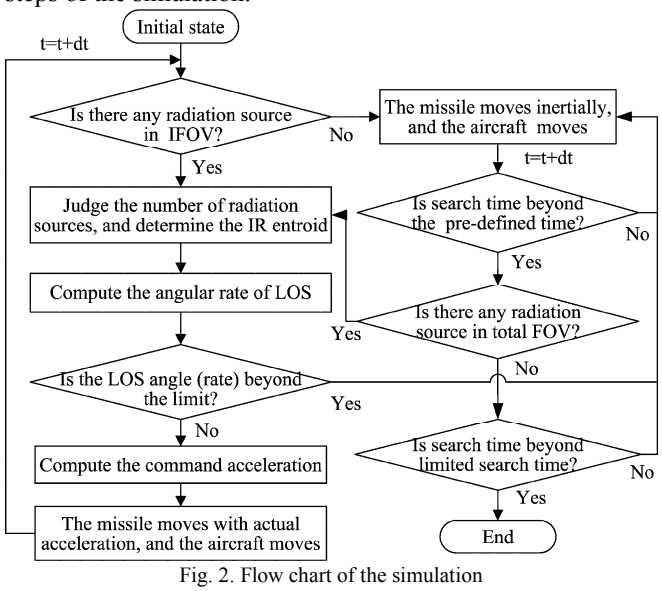

Fig. 2. Flow chart of the simulation

B. Engagement scenario

Considering a three-dimensional intercept situation, an aircraft at certain altitude is flying straight and level at

constant speed of V_t. At the same time, a missile is attacking the aircraft from an initial aspect angle α.

There are two parameters in the simulated engagement scenario shown in Fig.3.

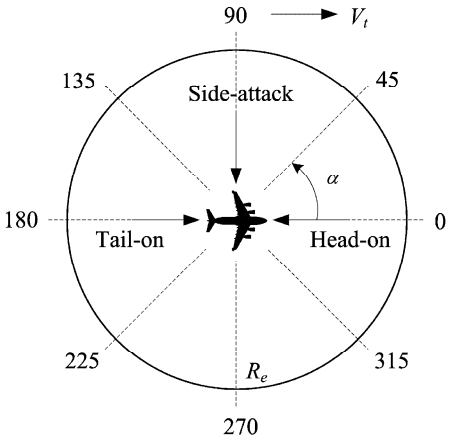

Fig. 3. Scenario sketch

1) Initial aspect angle α, which is the missile initial attacking angle. The angle α varies from 0deg (head-on), through 90deg (side-attack), to 180 deg (tail-on).

2) Dispensing range R. It is the distance between the aircraft and the missile when the aircraft detects the threat and starts deploying flares. R covers the range from 0 to R_e(km) in steps of ΔR =0.2km.

In Fig.3, each combination of two parameter values, (α, R), represents one simulated engagement scenario. For example, (180deg, 10km) means the flares are ejected when the missile is 10km away from the aircraft, for the missile with attacking angle of 180deg (from tail-on).

C. Criteria of successful decoy

1) In a flight simulation with a certain dispensing range, miss distance is the basis for evaluating the effect of the flare [10]. There is a cutoff miss distance D_0. A miss distance less than D_0 is accounted as a direct hit, which is defined as "no decoy," whereas a miss distance more than D_0 is considered as "successful decoy." D_0 can be taken as the maximum value between the missile kill radius and half the wing span of an aircraft.

2) The first criterion described above only fits for a certain dispensing range. However, in the actual engagement, the dispensing range is a random variable, which depends on the threat information provided by missile warning receiver. The jamming effectiveness is considered to be good when the miss distances are larger than D_0 under most dispensing ranges.

Hence, the probability of successful decoy, $P(J)$, is proposed to evaluate the effectiveness of a dispensing manner in a certain engagement scenario. Suppose the continuous miss distance curve due to dispensing range is illustrated in the following figure.

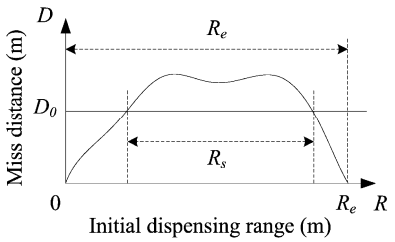

Fig. 4. Continuous miss distance curve

In Fig. 4, the miss distances corresponding to range interval of R_s are larger than D_0, so it means "successful decoy." Otherwise, out of this range interval, the miss distances are smaller than D_0, so it means "no decoy."

$P(J)$ is defined as the ratio of the range corresponding to "successful decoy" to the whole flight range R_e.

$$P(J) = \frac{R_s}{R_e}. \tag{3}$$

In the actual simulation, the dispensing range is discrete, and R_e=(N_e-1)·ΔR. The miss distance corresponding to each dispensing range, R, is calculated, and the discrete miss distance curve is illustrated in Fig. 5.

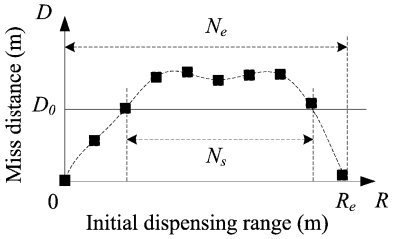

Fig. 5. Discrete miss distance results

So $P(J)$ can be rewritten in

$$P(J) = \frac{N_s - 1}{N_e - 1}, \tag{4}$$

where N_s represents the number of successful decoy, and N_e is the total simulation number.

VI. Examples and Discussions

It is assumed that an aircraft at the altitude of 4km is flying at the speed of V_t=272m/s, and the infrared radiation intensity of the aircraft I_t=2000W/sr. Meanwhile, a missile located on the ground may engage with the aircraft, and the flight distance R_e=10km. The missile speed keep constant at V_m=650m/s. The parameters associated with the missile guidance loop are listed in Table 1.

TABLE I

PERFORMANCE PARAMETERS OF THE MISSILE

IR seeker	Time constant T_1	0.05 s
	IFOV angle	3 deg
	Total FOV angle	45 deg
	Maximum LOS angular rate	20 deg/s
Guidance system	Navigation ratio N'	4
	Time constant T_2	0.15 s
Flight control system	Natural frequency ω_m	12 rad/s
	Damping factor ζ_m	0.6
	Limit of acceleration	31 g

The typical parameter values of the flares are set as follows: the peak intensity I_{MAX} is 4000W/sr, and t_{TOP}=0.5s, t_{MAX}=0.5s, t_{LAST}=5s; the original flare mass is 0.5kg, and the consuming speed is 0.1kg/s. The flare is launched backwards with respect to the aircraft at the speed of 30m/s. 30 flares are deployed in each engagement with time interval Δt.

Additionally, D_0 is taken as 25m (half the wing span of an aircraft) in this example.

A. Miss distance due to different time intervals.

For head-on intercept situation, the miss distances due to dispensing ranges at different intervals are plotted, as shown in Fig. 6.

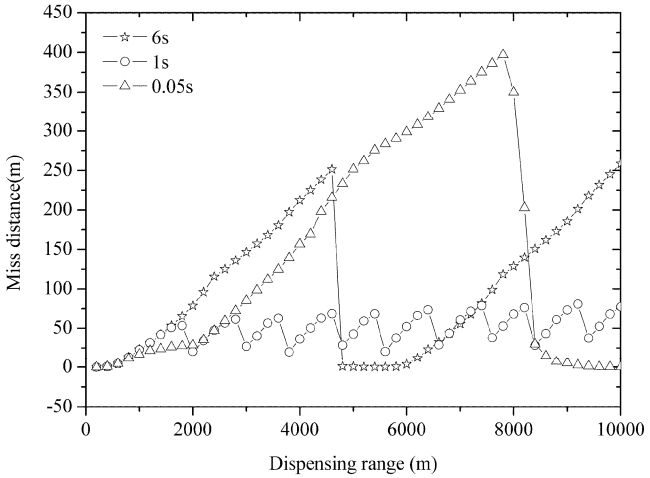

Fig. 6. Miss distances due to dispensing ranges (head-on)

According to the results, it is demonstrated that:

1) When the time interval is larger than the flare's burn time, that is Δt=6s, and $\Delta t > t_{LAST}$.

In this situation, after one flare burns out, the next flare will not come up in seeker's IFOV immediately. So the missile will search the aircraft and track it again until the next flare is dispensed. Consequently, the effect of the previous flare is eliminated, and the miss distance depends on the function time of the newest flare. The longer the function time is, the larger the miss distance. This is the reason of the periodic fluctuation of the curves in Fig.6. For the curve corresponding to Δt=6s, the fluctuation period is about 6s, which is equal to the time interval Δt.

2) When the time interval is smaller than the flare's burn time, that is Δt=1s, and $\Delta t < t_{LAST}$.

In this situation, the flares will function in the whole guidance process. In a long period, the newest flare always keeps in the IFOV, so the missile will track the centroid until the intercept occurs. Hence, the miss distance due to this is relatively stable. Whenever the flare is dispensed, it will cause a miss distance large enough to seduce the missile. For the curve corresponding to Δt=1s in Fig.6, the fluctuation period is about 1s, which is equal to the time interval as well.

3) When the time interval is very short (Δt =0.05s), which means Δt is nearly equal to zero.

If the time interval is too short, the flares will burn out earlier before the intercept. So the miss distance due to this is different from the results mentioned above.

Let Δt =0, which means simultaneous dispensing of a large number of flares, and is referred to dispensing in salvo. And then the miss distances due to different dispensing ranges for head-on intercept situation are plotted, as shown in Fig. 7.

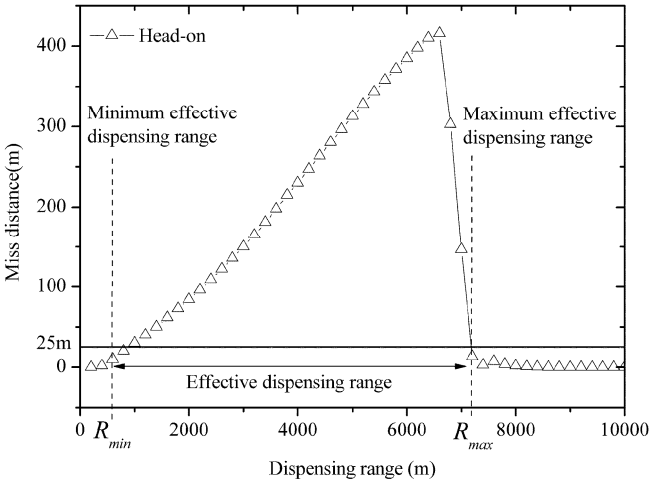

Fig. 7. Miss distance as a function of dispensing range

The curve in Fig.7 shows that there are two cutoff ranges R_{min} and R_{max} , and the miss distances between them are larger than 25m.

When flares are dispensed at the range further than 7.2km, they can decoy the missile sufficiently at first. But after the flares burned out, the missile is still in the guidance flight and there is no radiation source in the seeker's IFOV. So the seeker will search and acquire the aircraft again, then the missile will be controlled to fly towards it. Hence, the effect of the flares at the beginning is eliminated, which results in miss distances smaller than 25m, accounted as "no decoy." Besides, jettison at the range shorter than 0.9km makes the flare function time too short to drag away the missile effectively, so it results in "no decoy" as well.

Consequently, the cutoff ranges R_{min}, R_{max} are minimum and maximum effective dispensing range, respectively. When flares are ejected between R_{min} and R_{max}, they will last burning

until the missile guidance flight ends. The flares can decoy the missile continuously and effectively, and make it impossible for the seeker to track the aircraft again.

B. Optimum time interval for dispensing in burst.

The probabilities of successful decoy $P(J)$ due to Δt in three intercepts are calculated, as shown in Fig. 8.

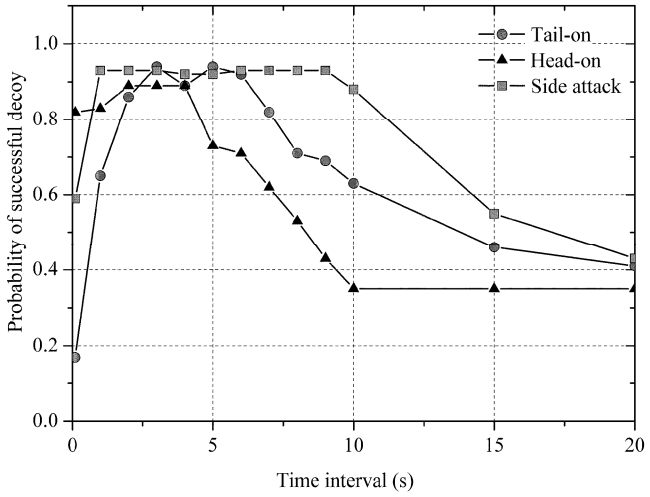

Fig. 8. Miss distances due to different time interval

It is shown that the probabilities of successful decoy increase firstly, and then decrease with the time interval Δt increasing. The results for side attack is not sensitive to Δt. From the point of view of successful decoy probability in three attacking aspects, the optimum time interval Δt can be derived, which is about 3s in this example.

C. Effective dispensing region for dispensing in salvo.

Although the successful decoy probability for salvo is smaller that that for dispensing at optimum time interval, the effect for salvo depends on the cutoff ranges severely, and the continuous effective dispensing range R_s is larger. So it benefits to the tactical use of flares in actual combat.

The miss distances as a function of dispensing range for different attacking aspects shown in Fig.3 are calculated. Then, the corresponding effective dispensing ranges are calculated and their envelopes are plotted.

Fig. 9 presents the effective dispensing region of the flares, which is the area between these two envelopes. The flares dispensed at the range between these two effective dispensing range envelopes can decoy the missile effectively.

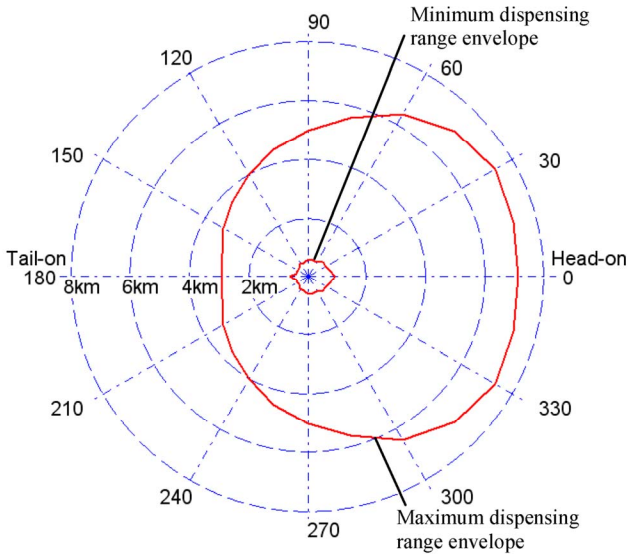

Fig. 9. Effective dispensing region

According to the two envelopes in Fig.9, it is demonstrated that the aircraft should deploy the flares at a longer range in head-on intercept, and at a shorter range in tail-on intercept. In this example, the maximum dispensing range in head-on and tail-on intercept are about 7km and 3km, respectively. The difference is mainly caused by the closing velocity between the missile and the aircraft.

In tail-on intercept, the closing velocity is lower than that in head-on intercept, so the flight time is longer. To avoid acquiring the aircraft again, the flares should be released at a shorter range in tail-on intercept compared with head-on intercept. That's why both the maximum and minimum effective dispensing ranges in tail-on intercept are shorter.

VII. CONCLUSION

A method is developed to evaluate the effectiveness of the flare when it is dispensed in burst.

The results have demonstrated that:

1) If the flares are dispensed in burst, and the time interval is larger than zero, the effect of flares is up to the time interval. When time interval is larger than flare burn time, the flare can not function continuously in the guidance flight. Form the point view of successful decoy probability, the optimum time interval can be derived, which is slightly smaller than flare burn time.

2) If the flares are dispensed in salvo, they should be deployed in certain region to achieve effective decoying. This region is denoted by an interval between the minimum and maximum effective dispensing range. Furthermore, the effective dispensing range changes with missile attacking aspects.

The studies performed on the effectiveness can be utilized, to propose the scientific suggestions for the tactical usage of airborne infrared flare. If the range information of the threat can be derived in the engagement, the flare should be ejected manually in the effective dispensing region to ensure decoying

the missile successfully. Otherwise, the flares can be ejected automatically with an optimum time interval to get a successful decoy probability as large as possible.

REFERENCES

[1] M. A. Richardson, N. Tranquillino-Minerva , B. Butters, R. Walmsleyb, R. Aylingb, N. Millwoodb, "Modeling the Improved Protection of Fast Jets from the IR MANPADS Threat", *Proceedings of SPIE*, Vol. 6397, 2006.

[2] J. Berggren R. Kihlén, "Model for simulation of IR countermeasure effect on IR-seeker/missile", *Proceedings of SPIE*, Vol. 5615, 2004, p.72-83.

[3] W. D. Jong, F. A. M. Dam, G. J. Kunz, Ric. M.A. Schleijpen, "IR seeker simulator and IR scene generation to evaluate IR decoy effectiveness", *Proceedings of SPIE*, Vol. 5615, 2004 ,p.100-111.

[4] D. Forrai, J. Maiter, "AIRSAM: A Tool for Assessing Airborne Infrared Countermeasures", Air Force Research Lab, NY, ADA458135, 2000

[5] D. P. Forrai, J. J. Maier, "Generic models in the advanced IRCM assessment model", *Proceedings of the 2001 Winter Simulation Conference*, pp. 789-796.

[6] D. H. Poollock, *"the Infrared & Electro-Optical Systems Handbook"*, in *Countermeasure Systems*, Vol.7, Bellingham, Washington: SPIE Optical engineering Press, 1999, pp.287-315.

[7] P. Zarchan. *Tactical and Strategic Missile Guidance*, 3rd ed., Reston, VA: American Institute of Aeronautics and Astronautics, Inc., 2002.

[8] A. E. Locke, *Guidance*, NJ: Van Nostrand Princeton, 1955.

[9] P. Garnell, D. J. East, *Guided Weapon Control System*, Elmsford, New York: Pergamon Press, 1977.

[10] R. E. Ball, *The Fundamentals of Aircraft Combat Survivability Analysis and Design*, 2nd ed., Reston, VA: American Institute of Aeronautics and Astronautics, Inc., 2003, ch. 4.